Pure appl. geophys. 159 (2002) 543–562
0033–4553/02/030543–20 $ 1.50 + 0.20/0

Pure and Applied Geophysics

Evaluation of Subsurface Structure at Soultz Hot Dry Rock Site by the AE Reflection Method in Time-frequency Domain

NOBUKAZU SOMA,[1] HIROAKI NIITSUMA[2] and ROY BARIA[3]

Abstract — Because the Soultz Hot Dry Rock (HDR) site, France, is to be expanded to a scientific pilot plant of greater depth, measurement of the deep area below the predeveloped artificial reservoir is gaining importance. In this paper, we present estimates of deep subsurface structure at the Soultz HDR site, obtained by a reflection method using acoustic emission (AE) signals, that is, induced seismicity, as the wave source. First, we briefly describe the AE reflection method in the time-frequency domain with wavelet transform. Then we show estimates of the subsurface structure by using 101 high-energy AE events observed in 1993. We compare and discuss the results obtained, using the AE reflection method in two wells with other independent borehole observations. Furthermore, we present the results of an investigation of the frequency dependence of reflectors identified by hodogram linearity as a possible means of further characterizing detected structures.

Key words: Reflected AE, linearity of three-dimensional hodogram, wavelet transform, time-frequency domain.

1. Introduction

The European Hot Dry Rock (HDR) programme is located at Soultz-sous-Forêts in northeastern France, some 50 km north of Strasbourg (Fig. 1). The site has been developed since 1987 with support from France, Germany, and the European Commission (EC) (BARIA *et al.*, 1995). In order to obtain geothermal energy from the deep crust, an artificial geothermal reservoir was created by hydraulic experiments. In the summer and autumn of 1997, a four-month long circulation test was conducted to demonstrate the possible future use of the HDR system as a renewable energy source. The test showed that the system had an acceptable production rate and negligible water losses, and required minimum input energy (BAUMGÄRTNER *et al.*, 1998). Since this successful test, development has proceeded to greater depths in order to reach temperatures high enough for practical use. One well, GPK2, was deepened from 3.5 km to 5.0 km in the spring of 1999.

[1] National Institute for Resources and Environment, 16-3 Onogawa, Tsukuba 305-0035, Japan. E-mail: n.soma@aist.go.jp
[2] Graduate School of Engineering, Tohoku University, Aoba01, Aoba-ku, Sendai 980-8579, Japan.
[3] SOCOMINE, Rute de Kutzenhausen BP39, F67250 Soultz-sous-Forêts, France.

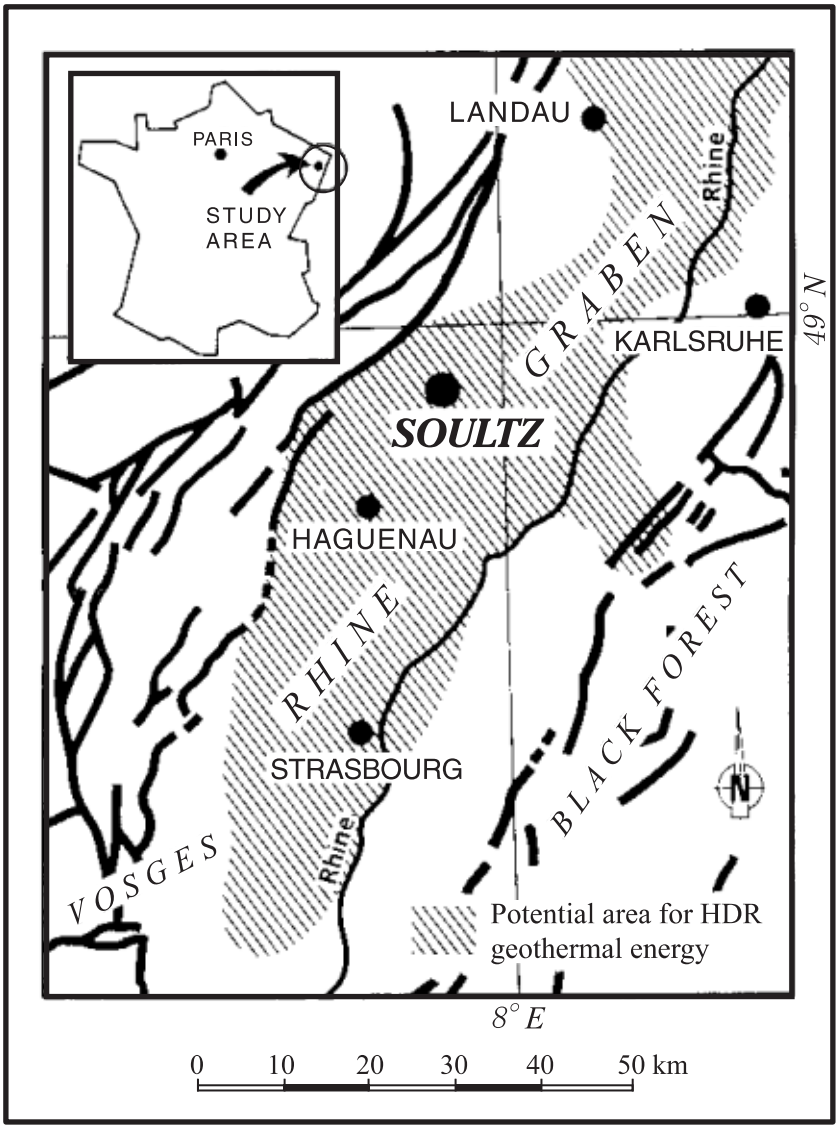

Figure 1
Location map of the Soultz HDR site.

In the Soultz project, induced seismicity, called acoustic emissions (AE), is commonly used to investigate the extension of the artificial reservoir or the exploitation flow path, or to model the connectivity between the injection and production well. However, induced seismicity, as the technique is generally employed, can measure conditions only in the area of the geothermal reservoir,

even though it is important to understand conditions beneath or adjacent to the reservoir if the HDR system is to be expanded for practical use. Thus far, there has been no suitable technique for exploring those regions of a geothermal field.

Therefore, we developed a reflection technique in which natural or induced seismicity can be used as the wave source. We call it the ''AE reflection method'' (SOMA and NIITSUMA, 1997; SOMA *et al.*, 1997). This method has the following advantages: (i) the seismic energy of AE is greater than that of the more usual artificial wave sources, so it is possible to detect waves reflected from great depths; (ii) seismic sources are located in the deep rock mass as an inverse VSP (vertical seismic profile), thus there is less attenuation of the reflected waves compared to a survey from the surface; (iii) the horizontal distribution of seismic sources is relatively wide with no topographical restrictions; (iv) since the method requires only a passive measurement system, it is much less expensive and thus more practical for long-term, continuous observations; (v) if the proper source distribution is available, the method may be able to detect subvertical structures such as faults, which are a difficult target for a conventional technique used from the surface; (vi) use of a downhole multi-component detector allows observation of an enormous number of events, making three-dimensional processing possible even with only one detector.

The AE reflection method was initially developed for the time domain, and we have previously demonstrated its possibilities in geothermal fields (SOMA and NIITSUMA, 1997; SOMA *et al.*, 1997), although the resolution was not sharp enough for practical development. We have recently enhanced the method by developing a method of analysis in the time-frequency domain with wavelet transform (SOMA, 1998). We can expect the following advantages from time-frequency domain analysis with the AE reflection method, compared with time domain analysis: (1) higher resolution and accuracy for the detection of reflected waves, owing to the characteristics of wavelet transform; (2) less ambiguity because the method, unlike time domain analysis, does not require use of the sliding-time-window technique, which time domain analysis is forced to use; (3) robustness against noise because it is possible to choose the frequency component to avoid noise in the analysis; and (4) it offers various possibilities for the development of further signal processing techniques for imaging and characterizing subsurface structures.

In this study we estimated the deep subsurface structure in the Soultz HDR site using the AE reflection method in the time-frequency domain. We describe the Soultz site and the AE observation method, including how to detect reflected waves and image subsurface structure using the AE reflection method. Then we show the estimates of the deep subsurface structure in the Soultz HDR site obtained using waveforms recorded in 1993. We also make precise estimates of the structure along two boreholes and compare them with other well observations. Finally, we discuss the frequency dependence of the detected reflectors in an effort to characterize the deep subsurface structure.

2. Soultz HDR Site and AE Observation

The geology of the Soultz HDR site consists of shallow sedimentary layers and a deep crystalline rock mass consisting mainly of granite below a depth of approximately 1400 m. There are two geothermal wells (GPK1 and GPK2), four seismic wells, and one exploration well. The geothermal well GPK1 was drilled to a depth of 3.5 km and several hydraulic experiments were conducted. In 1993 massive hydraulic fracturing was performed at depths between 2800 and 3500 m in well GPK1, to create an artificial geothermal reservoir inside the basement granitic rock. Next, a second well, GPK2, was drilled in the vicinity of the artificial reservoir and a circulation system was successfully developed in 1995 (BAUMGÄRTNER *et al.*, 1996). After the success of a four-month circulation test in 1997, GPK2 was deepened to 5 km in the spring of 1999, in order to obtain higher temperatures. However, there is as yet sparse information available from the deepened part of GPK2.

During the massive hydraulic fracturing in 1993, about 20,000 AE events were observed with four-component downhole detectors (JONES and ASANUMA, 1997) deployed inside the basement rock and recorded as digital data sets with a 5-kHz sampling frequency. From the 1993 data sets we selected for analysis 101 high-energy events, which had been recorded in unusually long files. Unfortunately, we were able to use data from only one detector, designated E4550 (Fig. 1), because we could not collect enough usable waveform data from the other stations. We did not have reliable and precise hodograms from the other stations, probably due to minor electrical trouble during the experiment. The source location of the events was determined using all detectors (DYER *et al.*, 1994), since that procedure is less sensitive to hodogram accuracy. The source locations of the 101 events and the orientations of the cross sections later used for the subsurface structure estimates are shown in Figure 2. A typical AE waveform can be converted into a conventional three-component signal (see, for example, Fig. 3). Each waveform used contained about 3.0 s of data, which is longer than the usual AE measurement in this field, so that deeper subsurface structures could be seen. The dominant frequency of the waveforms was around 200 Hz. Many AE events recorded a high signal-to-noise amplitude ratio (S/N). We could identify the arrival of direct *P* and *S* waves relatively clearly because the site geology is mostly granite, which has low attenuation and high frequency signals. However, it was impossible to discriminate reflected waves from observed waveforms directly because they were covered by coda.

3. Outline of the AE Reflection Method in the Time-frequency Domain

The AE reflection method has two parts: distinguishing reflected waves from coda by the hodogram technique, and three-dimensional inversion for imaging with

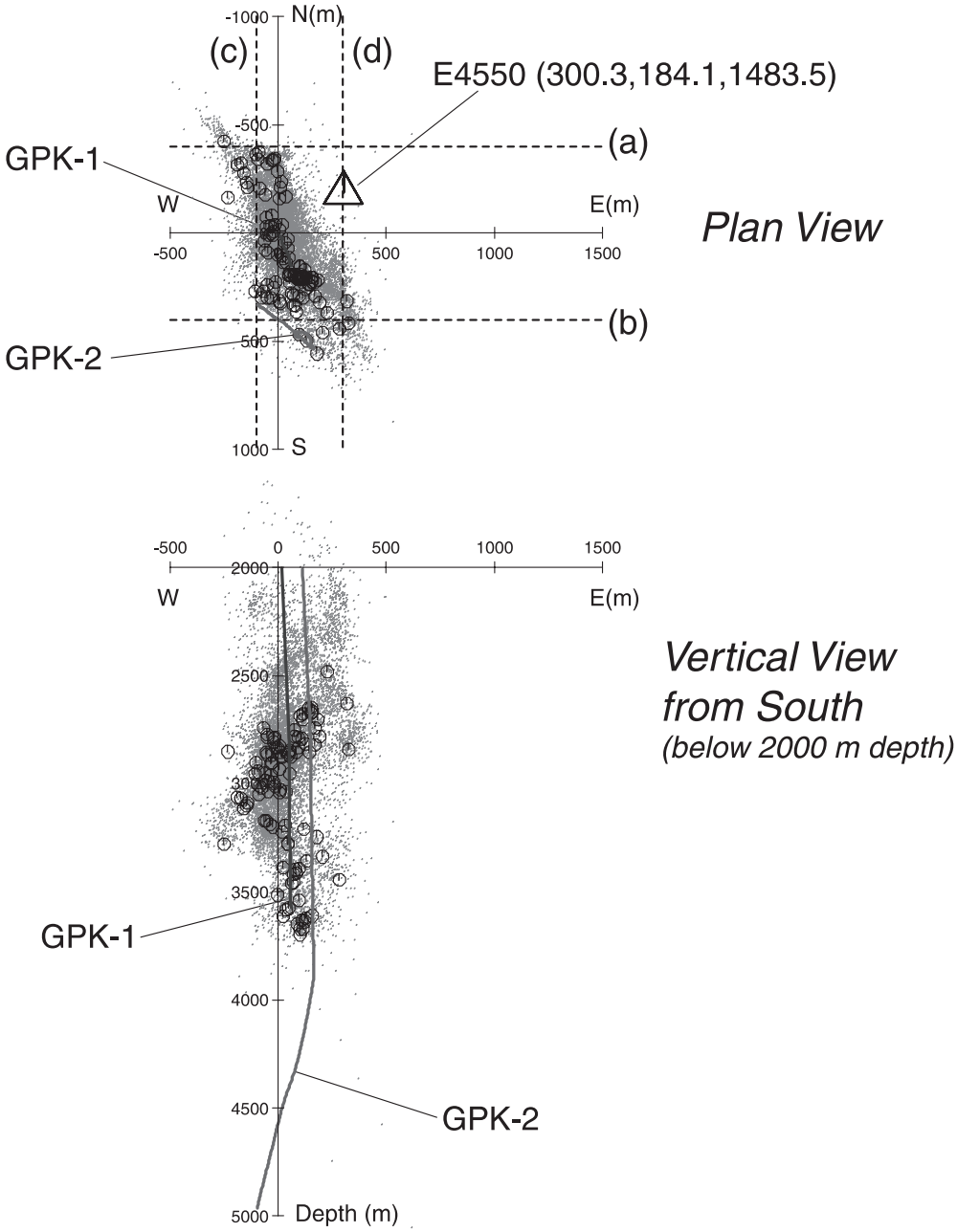

Figure 2

Source locations of the 101 AE events used for the analysis (circles). The triangle shows the detector at observation well E4550, and the gray cloud shows the distribution of all events observed in September, 1993. Trajectories of well GPK1 and well GPK2 which were deepened in 1999 are shown in the vertical section. Dotted lines in the plan view show the orientation of cross sections used for the estimates shown in Figure 5.

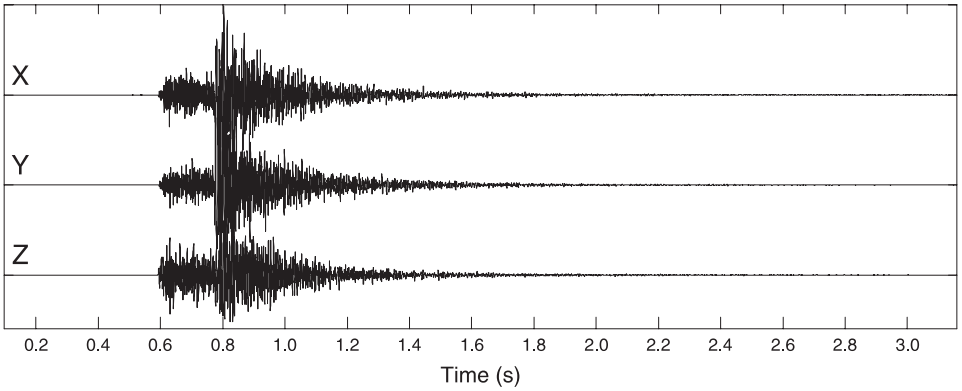

Figure 3
Example of a typical three-component AE waveform at the Soultz site.

a non-systematic source distribution (SOMA and NIITSUMA, 1997). We previously demonstrated in geothermal fields the potential of the method, which was initially developed for the time domain (SOMA and NIITSUMA, 1997; SOMA *et al.*, 1997). More recently we developed the time-frequency domain analysis method with wavelet transform in order to make this technique more practically useful (SOMA, 1998).

Because the reflected waves are covered by coda of the direct waves, conventional analysis based on wave energy or amplitude is useless for the analysis of reflected AE signals from a geothermal field. In the AE reflection method, the reflected waves are detected by investigating the shape of three-dimensional hodograms. The shape of the hodogram shows the trace of three-dimensional particle motion during the arrival of waves, and is known to indicate wave condition (NAGANO *et al.*, 1986). The shape of the hodogram is spherical when an incoherent signal such as random noise is detected, however it becomes relatively linear on the arrival of direct *P* or *S* waves, which are regarded as coherent signals (SOMA and NIITSUMA, 1997; SOMA *et al.*, 1997). In our study, reflected waves are regarded as coherent signals, since we assumed that the reflector has scale, and coda are normally regarded as incoherent signals (AKI and CHOUET, 1975). Therefore, using the AE reflection method we can distinguish reflected waves from coda by investigating the shapes of the hodograms.

For the quantitative evaluation of hodogram shape we used a covariance matrix method in the frequency domain, which is also called a spectral matrix (SAMSON, 1977). In this study we regarded the wavelet transform as a time-frequency signal representation (RIOUL and VETTERLI, 1991), which shows a smoothed time-varied spectral similar to a short-time Fourier transform (STFT) (HLAWATSCH and BOUDREAUX-BARTELS, 1992). Generally, a time-frequency signal representation allows us to compose a spectral matrix in the time-frequency domain (MORIYA and

NIITSUMA, 1996). Hence, we can define a spectral matrix $\mathbf{S}_{WT}(b, a)$ of the hodogram by using the wavelet transform as formula (1),

$$\mathbf{S}_{WT}(b,a) = \begin{pmatrix} W_{xx}(b,a) & W_{xy}(b,a) & W_{xz}(b,a) \\ W_{yx}(b,a) & W_{yy}(b,a) & W_{yz}(b,a) \\ W_{zx}(b,a) & W_{zy}(b,a) & W_{zz}(b,a) \end{pmatrix} , \tag{1}$$

where $W_{ij}(b, a) = W_i(b, a)W_j^*(b, a)$, a: frequency (scale), b: time (shift), $W_i(b, a)$: wavelet coefficient of i component, * : complex conjugate.

The spectral matrix is generally complex but always satisfies the conditions of a Hermitian matrix (MORIYA and NIITSUMA, 1996). We can treat this matrix as in the time-frequency domain since "scale" and "shift" in the wavelet transform correspond to "frequency" and "time," respectively. Then we can redefine Samson's global polarization coefficient, $Cp(b, a)$, (SAMSON, 1977) to be in the time-frequency domain, as follows:

$$C_p(b,a) = \frac{(\lambda_1 - \lambda_2)^2 + (\lambda_2 - \lambda_3)^2 + (\lambda_3 - \lambda_1)^2}{2(\lambda_1 + \lambda_2 + \lambda_3)^2} , \tag{2}$$

where $\lambda_i = \lambda_i(b, a)$ ($i = 1, 2, 3$; $\lambda_1 > \lambda_2 > \lambda_3$): eigenvalue of the matrix (1) for each time (shift: b) and frequency (scale: a).

By this parameter we can quantitatively evaluate the shape of the hodogram in the time-frequency domain; $Cp(b, a) = 1$ for an exactly linear hodogram and $Cp(b, a) = 0$ for a spherical hodogram. The arrival of coherent waves, such as reflected waves, should have a high Cp value. Hence, we can use a high value of the parameter $Cp(b, a)$ as an indicator of the arrival of reflected waves.

For imaging the subsurface structure, we established a three-dimensional inversion of the waveform which shows the time-frequency distribution of the linearity of the three-dimensional hodogram. Here we focused on only simple S-to-S-wave reflection because the energy of the S wave was dominant in our application and P-wave reflection may be concealed by the energy of the S wave.

The inversion concept is diagrammed in Figure 4. This inversion, which can generate a three-dimensional estimate from a small number of detectors, is based on a type of diffraction-stack migration as explained below. The inversion can create a deep subsurface image with data from only one detector if the source location has enough extension considering the objective area, although more detectors are better for accuracy and reliability.

[1] The linearity waveform $Cp(b, a)$, formula (2) of a three-dimensional hodogram in the time-frequency domain, is calculated. We can also obtain the polarization direction of the hodogram for each time and frequency component.

[2] We can assume the iso-delay ellipsoid for a delay $\Delta T(a_1)$ for scale "a_1", considering the detector, source, and path length. The virtual reflected points for $\Delta T(a_1)$ are located on the ellipsoid.

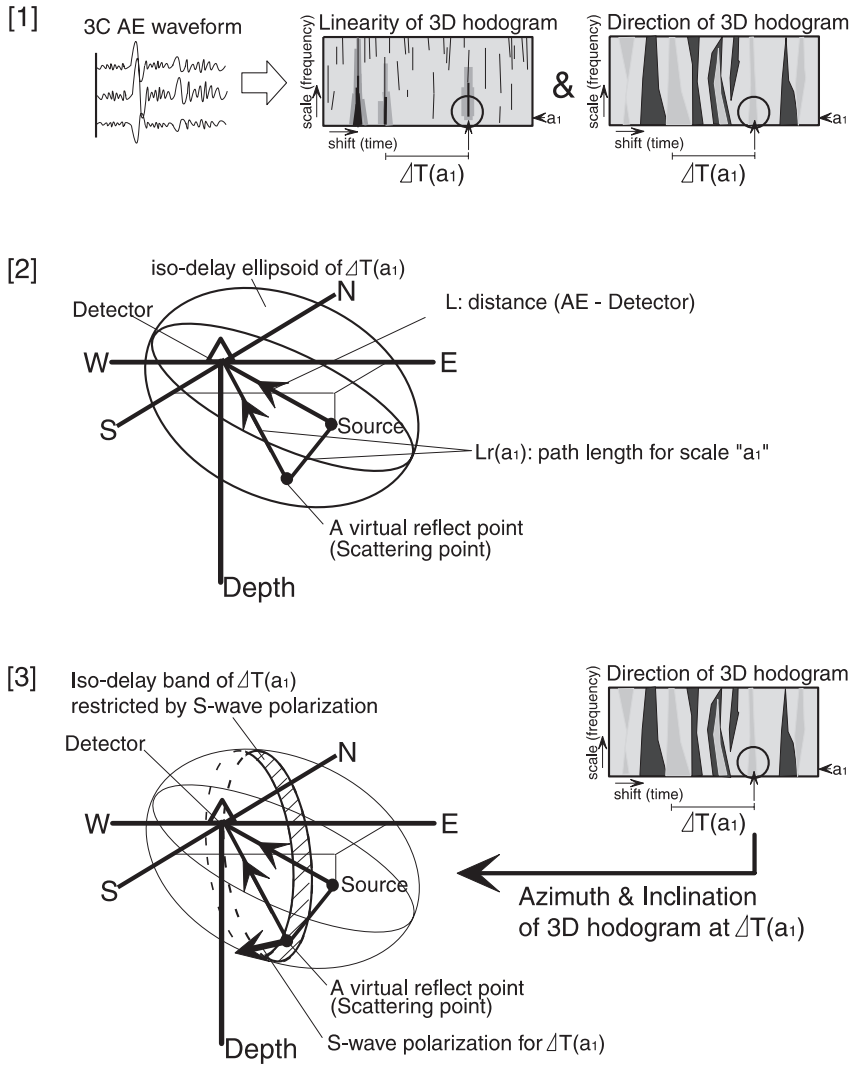

Figure 4
Diagram of the concept of three-dimensional inversion for the distribution of linearity of three-dimensional hodograms in the time-frequency domain.

[3] The strength of the linearity waveform for scale "a_1" is plotted on the ellipsoid.
[4] We repeat the process from [1] to [3] over all scales (frequency components) and all delays in the signal, and perform the same process for all of the usable AE events, after which the results are stacked.

In the inversion, we enhanced the resolution by restricting the virtual reflected points by examining the orthogonality between the propagation direction and *S*-wave polarization. The area in which the virtual reflected point occurs, where the strength

of hodogram linearity is plotted, can be reduced if we select the area where *S*-wave motion is perpendicular to the propagation direction from the reflected point when we focus on a *S*-to-*S*-wave reflection. By this process, the virtual reflected point can be restricted to a band as in step [3] of Figure 4.

In addition, the effect of heterogeneous source distribution is compensated for by normalizing wave density for numerous nearby events for each source. The heterogeneity of source distribution causes the final image to have a dominant ellipsoidal artifact, which comes from a center of source distribution. Normalization can reduce the effect of the ellipsoidal artifact (SOMA and NIITSUMA, 1997). These two operations are effective when the inversion uses a natural distribution of induced seismicity.

The actual signal processing is done with time and frequency steps, since digitalized data sets are used. In this study, each time step was about 0.2 ms, corresponding to the sampling frequency during data acquisition, and we set seven frequency steps from 39.9 to 317.1 Hz for the wavelet analysis.

4. Three-dimensional Estimates at the Soultz HDR Site

We estimated the deep subsurface structure at the Soultz HDR site by the AE reflection method with the 101 high-energy events from 1993. The estimates obtained for the E-W and N-S cross sections are shown in Figure 5. The estimates were obtained from an E-W cross section 400 m north of the wellhead of injection well GPK1 (Fig. 5a), an E-W section 400 m south of GPK1 (Fig. 5b), a N-S section 100 m west of GPK1 (Fig. 5c), and a N-S section 300 m east of the well (Fig. 5d). The result obtained by time domain analysis from the same section as shown in Figure 5d was used for comparison with the time-frequency domain analysis results (Fig. 5e) (SOMA *et al.*, 1997). In the figure, darker colors indicate a higher value of stacked hodogram linearity, which is regarded as reflectivity in the analysis.

The time-frequency domain analysis showed a higher resolution and a better ability to detect reflectors than did the time domain analysis. A reflector at a depth of about 3000 to 3500 m was clearly seen using the time-frequency domain analysis (Fig. 5d), but was blurred in the time domain analysis because it was very close to the depth of the source distribution (Fig. 5e). The reflector seen at about 4000 m depth in the time domain analysis (Fig. 5e) was detected as two separate images at depths of 3950 m and 4200 m by the time-frequency domain analysis (Fig. 5d), suggesting that the resolution of the time-frequency domain analysis was higher. Deep reflectors below 4500 m depth were also detected more clearly than with the time domain analysis. The improved performance of the time-frequency domain analysis makes precise comparisons with other borehole observations possible.

However, the detected reflectors shown in Figure 5 appear curved because of the non-ideal and limited observation conditions. Since we were able to use only one

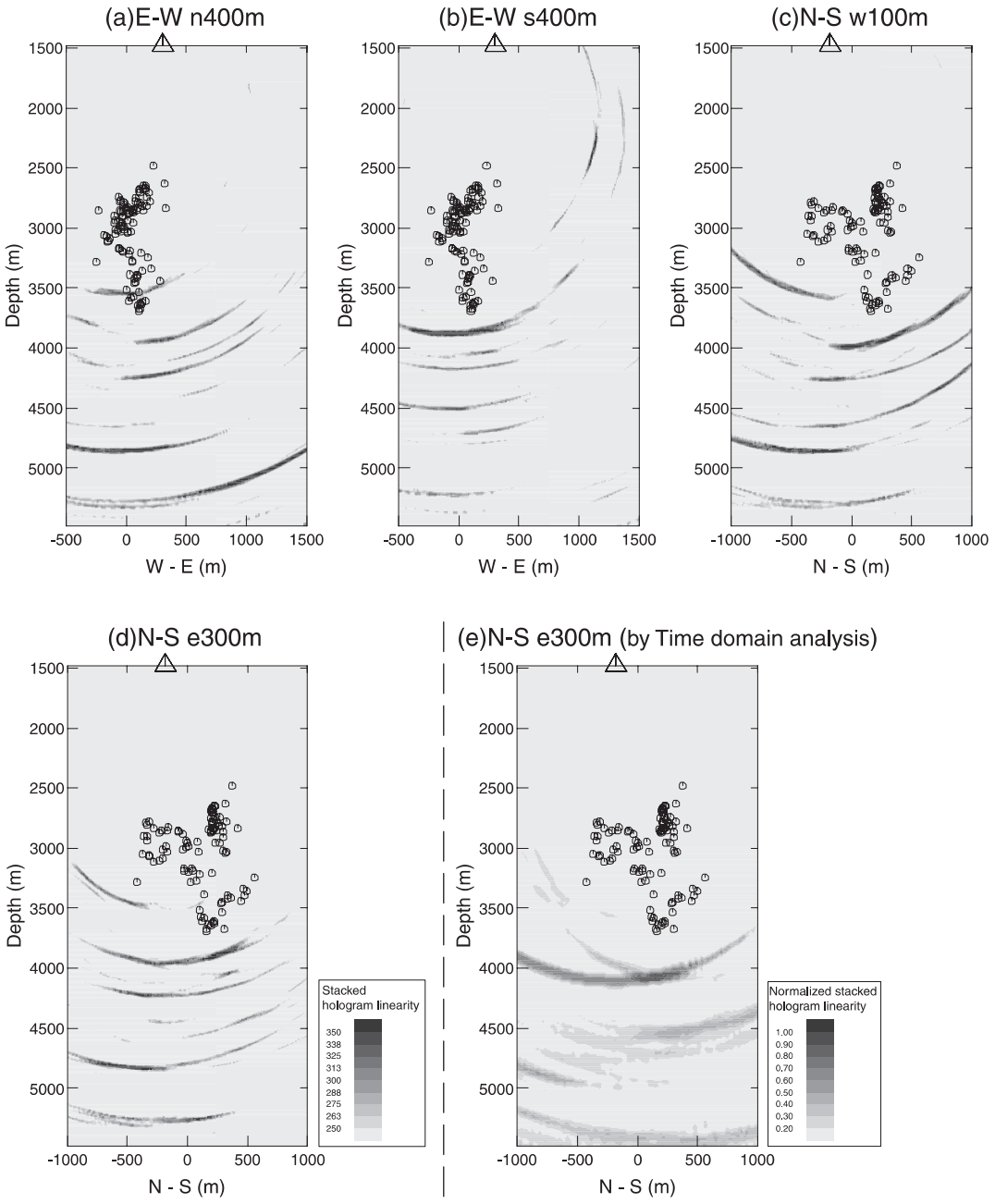

Figure 5
Cross sections of three-dimensional subsurface imaging by the AE reflection method in the time-frequency domain. (a): E-W cross section 400 m north from GPK1, (b): E-W section 400 m south, (c): N-S section 100 m west, (d): N-S section 300 m east, and (e): N-S section 300 m east analyzed in the time domain. The triangle and circles show the projections of the detector and sources, respectively.

detector, there was a strong geometrical effect. Therefore, we will not discuss the orientation or shape of the detected reflectors, but limit our discussion to the depth of the reflectors. We can roughly define the depth of each reflector using the point along the curved shape having the highest value, although the curved shape of the reflector affects the accuracy with which the depth can be determined. Thus reflectors were detected at depths of about 3500 m, 3950 m, 4200 m, 4500 m, 4800 m, and 5200 m.

The reflectors at 3950 or 4200 m depth may show the bottom of the artificially created reservoir because fracture conditions can be expected to change markedly there. To interpret the other reflectors, it is necessary to compare them carefully with other information collected independently.

5. Comparison with Other Borehole Data Sets

Since the AE reflection method generates three-dimensional volumetric results, we can estimate the subsurface structure wherever we choose. In order to make precise comparisons with borehole observations, we chose to make our estimates exactly along the trajectories of boreholes GPK1 and GPK2. Changes in hodogram linearity with depth (Fig. 6a), calculated from the AE reflection data and assumed to indicate reflectivity, were compared with several types of independent observations: the number of fractures per 10 m, based on formation micro-imager (FMI) log data (Fig. 6b), acoustic impedance log data (Fig. 6c), thermal flow meter log data (Fig. 6d), and helium log data (Fig. 6e). Hodogram linearity values at greater depths are larger because fewer events at shallow depths are usable if errors arising from the influence of direct waves are to be avoided. Therefore, data shown in the figure from depths shallower than 3100 m were considered unreliable and were disregarded.

Several major peaks in hodogram linearity indicated reflectivity at depths of 3100 m, 3200 m, 3330 m, 3375 m, 3500 m, and 3520 m (Fig. 6a) and agreed well with the fracture density data (Fig. 6b). The variations in the acoustic impedance log data also corresponded to the peaks obtained using the AE reflection method (Fig. 6c). These results suggest that the AE reflection method can detect fractures or fracture zones.

Thermal flow meter and helium log data are indicators of permeability. Major permeable zones in GPK1 occurred at depths of about 3192 m to 3293 m, 3370 m to 3406 m, and 3489 m to 3496 m (BARIA *et al.*, 1994). These zones were clearly detected in the AE reflection data. However, at present it is not possible to determine directly from AE reflection data whether or not a reflector indicates a permeable zone.

Hodogram linearity data were also collected in the deep portion of GPK2 (Fig. 7a), and compared with a geological section constructed from a synthetic petrographic log obtained from microscopic examination of drilling cuttings (GENTER *et al.*, 1999). The hodogram linearity was calculated from the AE reflection

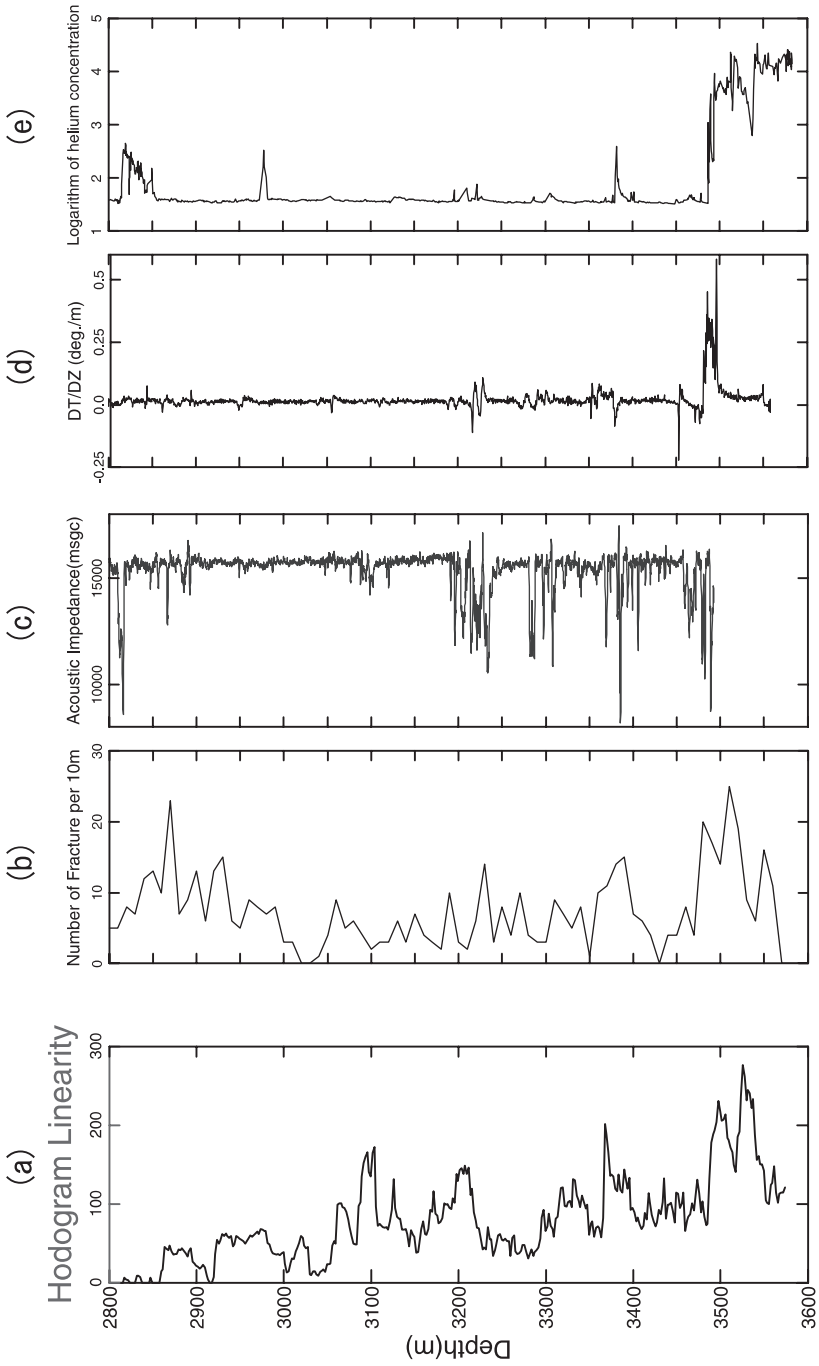

Figure 6

Comparison between the AE reflection method and other borehole observations in GPK1. (a): Estimation along GPK1 by the AE reflection method, (b): Number of fractures per 10 m based on FMI logging, (c): Acoustic impedance logging, (d): Thermal flow meter logging, and (e): Helium logging.

data before the actual drilling, and we adjusted the estimates to the actual well trajectory of the deepened borehole after well completion.

The AE reflection data showed probable reflectivity at depths of 3850 m, 4000 m, 4150 m, 4550 m, 4720 m, 4780 m, 4850 m, and 4950 m. Based on the relationships observed in GPK1, these results may indicate naturally existing structures such as fracture zones at great depth, since the data sets used were collected in 1993, before any hydraulic stimulation at these depths had been attempted.

The possible existence of many fracture zones has been reported, based on the microscopic examination of drilling cuttings obtained during GPK2 deepening (GENTER *et al.*, 1999). Major fracture zones composed of very highly altered granite were found at depths of about 4575 m and 4775 m. The most attractive permeable zone for the next phase of the project may be found at these depths because they will be helpful for developing a new deep artificial reservoir.

The AE reflection method clearly detected reflectors at depths of 4550 m and 4780 m, which correspond well to the two highly altered fracture zones found by examination of the drilling cuttings. Other peaks also appear to correspond to depths at which there was indication of the presence of other fracture zones. Therefore, there may exist many fracture zones at great depth at the Soultz HDR site. Accordingly, we can expect that deep HDR development at the Soultz site will be similar to development already completed at shallow depths.

6. Frequency Dependence of Detected Reflectors

In an attempt to characterize the detected structures, we examined the frequency dependence of hodogram linearity at each reflector depth. Since the AE reflection method is processed in the time-frequency domain, we can easily calculate frequency dependence. In this study we did not analyze the frequency dependence of wave amplitude but that of hodogram linearity, because the evaluation of wave amplitude covered by coda is too complicated. We investigated total hodogram linearity at each reflection point for each frequency component. Then we normalized it by the time resolution of each frequency component in a three-dimensional inversion.

The distribution of normalized hodogram linearity shows the frequency dependence of the estimate of subsurface structure (Fig. 8). Depth is shown on the vertical axis and the frequency component between 39.9 and 317.1 Hz is shown on the horizontal axis. The original hodogram linearity data are shown alongside. As before, data from depths less than 3100 m were disregarded.

Clear variations in frequency dependence among reflectors were observed in GPK1. For example, at depths of about 3100 m, 3200 m, 3520 m, the reflectors showed a tendency for lower frequency components to have more linear hodograms. On the other hand, the reflector at a depth of approximately 3400 m showed

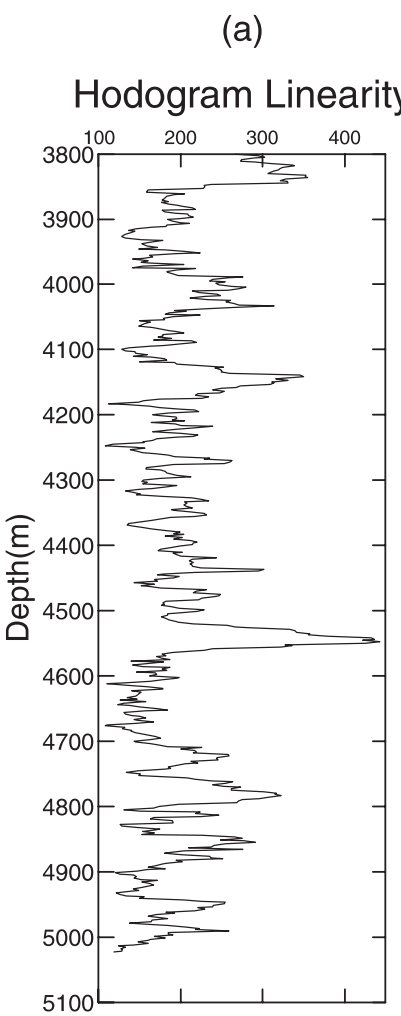

Figure 7
Comparison between the AE reflection method and drilling cuttings analysis in the deep well GPK2. (a): Estimation by the AE reflection method along the new well trajectory of GPK2 drilled in early 1999, (b): Synthetic log of GPK2 between 3880 and 5090 m depth according to analysis of the cuttings (GENTER *et al.*, 1999).

hodogram linearity in the middle- to high-frequency range. This kind of variation probably is related to the character of the structure since the nature of the reflection is a function of wavelength.

Some differences among the four reflectors were evaluated by a precise examination of borehole data sets. The fracture zones at about 3100 m, 3200 m, and 3520 m depth are known to have major flow, although major flow has not been found at 3400 m (EVANS, 2000). This difference may be shown by the frequency

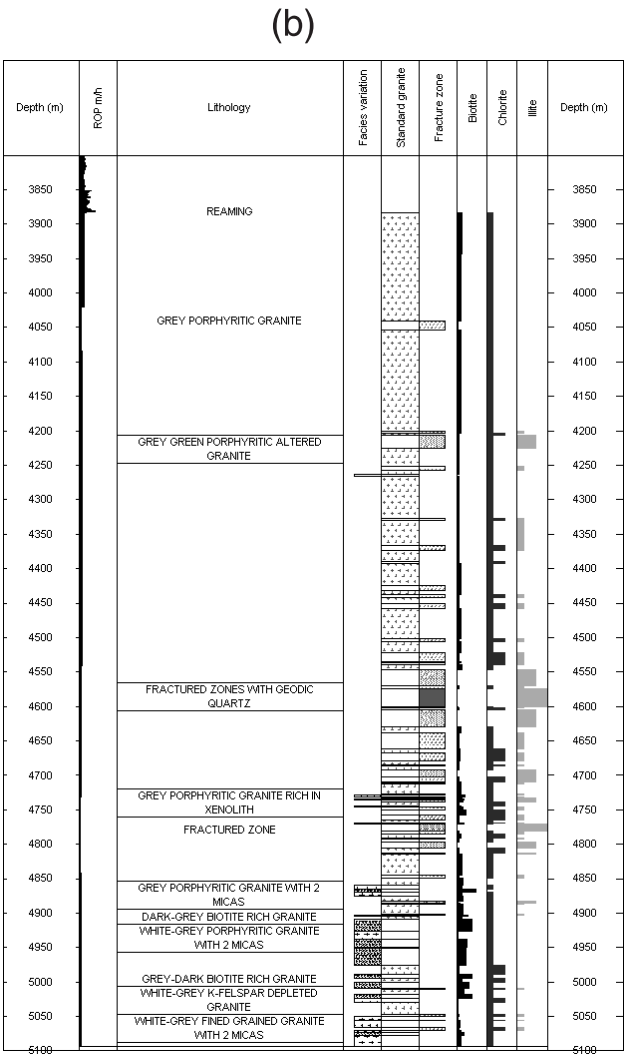

Figure 7b

dependence of hodogram linearity. The reflector with a higher frequency component may be a less permeable structure.

In the context of the Soultz HDR project, we assume that permeability is increased by the shearing and jacking of fractures. Thus, if the surface of a fracture is rough, the permeability of the fracture may be higher. Another possible source of high permeability is a multifracture zone. Furthermore, the extent of the fracture also affects permeability. These possible origins of permeability are also important factors affecting wave reflection.

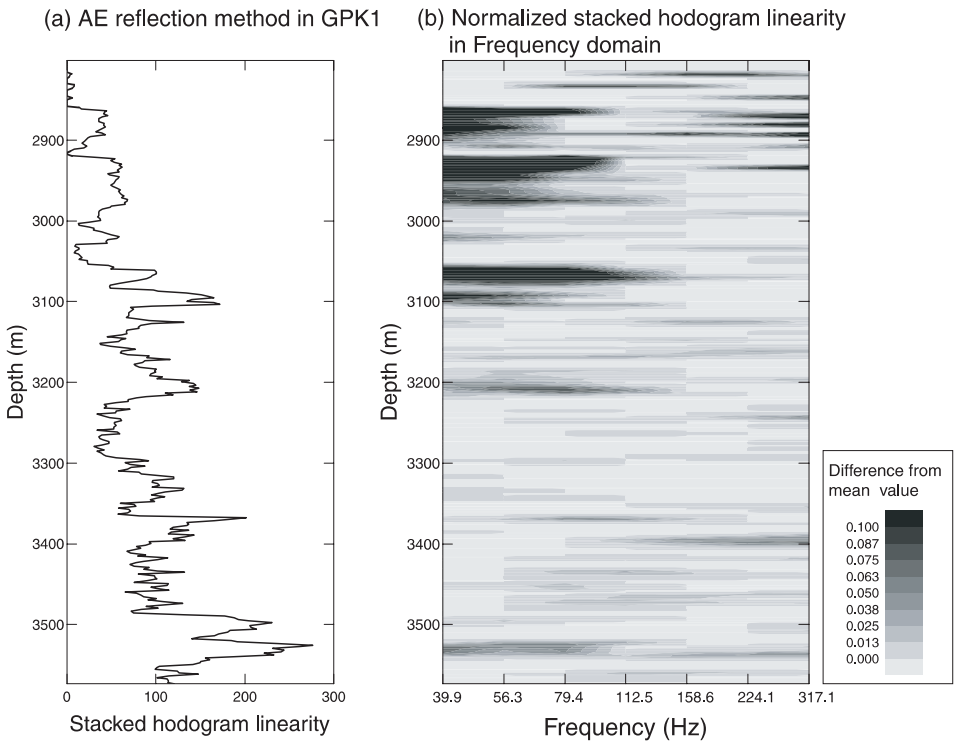

Figure 8
Estimate by the AE reflection method and frequency dependence of reflectors in GPK1.

Considering such permeability in the HDR system, the higher frequency component is greatly affected and is seen as a random nonlinear hodogram at a highly permeable reflector. The lower frequency component, conversely, can be reflected if the reflector is of considerable enough extent. Frequency dependence mainly reflects the shape of the surface and extent of the fracture, which relates to permeability in the context of the Soultz HDR site because the frequency dependence here does not relate to wave energy but to the shape of a three-dimensional hodogram with normalized wave energy.

However, the mechanism by which frequency affects the shape of the hodogram is not yet clear. Possible explanations for the frequency dependence include the physical properties of the material within the fracture and differences in the elastic properties of materials across the fracture. Further study is necessary to conclude the mechanism of frequency dependence of the shape of the three-dimensional hodogram.

Most of the reflectors in the deep part of GPK2 displayed middle to high frequency dependence (Fig. 9), except for those at 4100 m and 4500 m depth. This pattern implies that most of the fracture zones are less permeable than those in

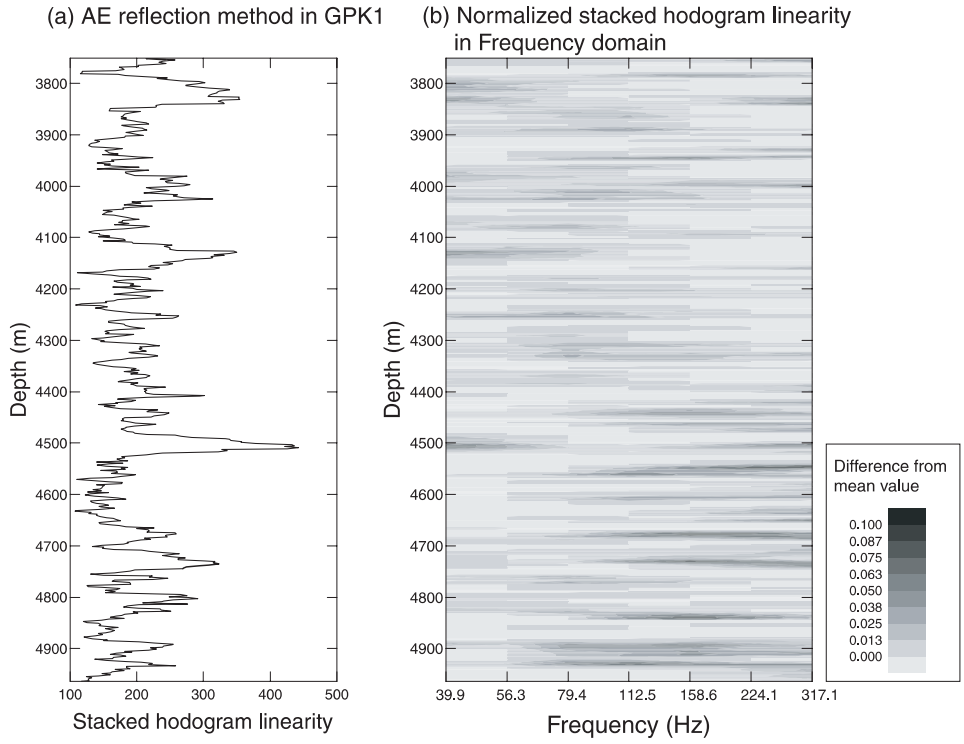

Figure 9
Estimate by the AE reflection method and frequency dependence of reflectors in the deepened part of GPK2.

GPK1 because the estimates were calculated under prestimulation conditions. The reflectors showing lower frequency dependence may be zones with relatively high permeability under predeveloped conditions. These may be promising zones for the next deep development project. Moreover, after the next large-scale fracturing, some reflectors with high frequency dependence may be expected to change to lower frequency dependence, if some natural fracture zone becomes activated as a dominant flow path.

Thus, this technique for analyzing the frequency dependence of reflectors is useful for characterizing deep subsurface structure in geothermal fields.

7. Conclusion

We estimated the deep subsurface structure at the Soultz HDR site by the AE reflection method in the time-frequency domain where natural or induced seismicity was used as a wave source. We compared data obtained using the AE reflection

method in two boreholes with other independent borehole observations. We also examined the characteristics of the reflectors by an analysis of frequency dependence.

First we detected several deep reflectors on the general three-dimensional image, although the shape of reflectors was distorted due to artifacts related to the limited observation conditions. The reflector corresponding to the bottom of the artificial reservoir may have been detected as well.

For the further interpretation of deep subsurface structures, we estimated the linearity of three-dimensional hodograms, assumed to indicate reflectivity in our analysis, along the well trajectories of GPK1 and the deepened part of well GPK2. Then we compared estimates obtained by the AE reflection method with other borehole data. In GPK1, we found that the detected reflectors corresponded to the distribution of fracture density based on FMI log data as well as to peaks in acoustic impedance log data. Therefore, the AE reflection method can be used at the Soultz HDR site to show the distribution of fracture zones.

The estimate in the deepened well, GPK2, also showed many peaks in hodogram linearity, indicating reflectivity. We assume that these peaks correspond to fracture zones at great depths prior to hydraulic stimulation. The structures estimated using the AE reflection method corresponded to fracture zones reported from the analysis of drilling cuttings. Therefore, fracture zones may exist at great depths at the Soultz HDR site as well as at shallow depths. Consequently, there seems to be potential for successful deep development at the site.

We also investigated the frequency dependence of reflectors detected by hodogram linearity in GPK1 and GPK2. There is clear variation in the frequency component at each reflector position. Although the mechanism of frequency dependence is not yet clear, this study suggests the possible utility of the method to characterize deep subsurface structures. Lower frequency dependence appears to be associated with reflectors at depths of known major flow zones, and not to be associated with reflectors where low permeability has been found.

The AE reflection method can potentially provide us substantial information regarding subsurface structure in areas adjacent to or below the reservoir of a geothermal field, where it is difficult to employ conventional survey methods. Since the analyses are done using *S*-wave polarization, the method is more sensitive to the detection of thin structures such as fracture zones than normal *P*-wave amplitude analysis. With a better observation network, the AE reflection method is likely to provide a more reliable and precise three-dimensional image, which will be very useful for practical subsurface development.

Acknowledgments

This work was carried out as a part of the MTC Project and MURPHY Project, both of which are supported by the New Energy and Industrial Technology

Development Organization (NEDO), Japan (International Joint Research Grant). This work was also supported in part by the Japan Society for the Promotion of Science (Grant JSPS-RFTF 97P00901). We would also like to thank SOCOMINE for providing the data from the European HDR site at Soultz-sous-Forêts, which is supported mainly by the European Commission, BMBF (Germany), and ADEME (France).

References

AKI, K. and CHOUET, B. (1975), *Origin of Coda Waves: Source, Attenuation and Scattering*, J. Geophys. Res. *80*, 3322–3342.

BARIA, R., BAUMGÄRTNER, J., GÉRARD, A., and JUNG, R. (1994), *Scientific Results Associated with Large-scale Hydraulic Injection Tests (A Summary of the Scientific Programme Carried out in 1993; 11/1/94). The European Geothermal Energy Project at Soultz-sous-Forêts*, Socomine Internal report.

BARIA, R., GARNISH, J., BAUMGÄRTNER, J., GÉRARD, A., and JUNG, R. (1995), *Recent Developments in the European HDR Research Programme at Soultz-sous-Forêts (France)*, Proc. World Geothermal Congress, 1995, Florence, Italy, International Geothermal Association, vol. 4, pp. 2631–2637, ISBN 0-473-03123-X.

BAUMGÄRTNER, J., JUNG, R. GÉRARD, A., BARIA, R. and GARNISH, J. (1996), *The European HDR Project at Soultz-sous-Forêts: Stimulation of the Second Deep Well and First Circulation Experiments*, Proc. 21st Workshop Geothermal Reservoir Engineering, Stanford University, Stanford, California, SGP-TR-151, pp. 267–274.

BAUMGÄRTNER, J., GÉRARD, A., BARIA, R., JUNG, R., TRAN-VIET, T., GANDY, T., AQUILINA, L., and GARNISH, J. (1998), *Circulating the HDR Reservoir at Soultz: Maintaining Production and Injection Flow in Complete Balance – Initial Results of the 1997 Circulation Experiment*, Proc. 23rd Workshop Geothermal Reservoir Engineering, Stanford University, Stanford, California, SGP-TR-158.

DYER, B., JUPE, A., JONES, R. H., THOMAS, T., WILLIS-RICHARDS, J., and JAQUES, P. (1994), *Microseismic Results from the European HDR Geothermal Project, Soultz-sous-Forêts, Alsace, France – 1993*, CSM Associates Limited, Internal report.

EVANS, K. (2000), *The Effect of the 1993 Stimulations of well GPK1 at Soultz on the Surrounding Rock Mass: Evidence for the existence of a Connected Network of Permeable Fractures*, Proc. World Geothermal Congress, 2000, Japan (in press).

GENTER, A., HOMEIER, G., CHEVREMONT, Ph., TENZER, H. (1999), *Deepening of GPK-2 HDR Borehole, 3880–5090 m, (Soultz-sous-Forêts, France). Geological Monitoring*, BRGM Open File Report, R 40685, 40 pp.

HLAWATSCH, F. and BOUDREAUX-BARTELS, G. F., (1992), *Linear and Quadratic Time-frequency Signal Representations*, IEEE Signal Processing, April, 21–67.

JONES, R. and ASANUMA, H. (1997), *Analysis of the Four-component Sensor Configuration*, MTC/NEDO Internal Report, vol. 2.

MORIYA, H. and NIITSUMA, H. (1996), *Precise Detection of a P-wave in Low S/N Signal by Using Time-frequency Representations of a Triaxial Hodogram*, Geophysics *61* (5), 1453–1466.

NAGANO, K., NIITSUMA, H., and CHUBACHI, N., *A new automatic AE source location algorithm for downhole triaxial AE measurement*. In *Progress in Acoustic Emission III* (eds. Yamaguchi, K. *et al.*) (The Japanese Soc. for NDI 1986) pp. 396–406.

RIOUL, O. and VETTERLI, M. (1991), *Wavelets and Signal Processing, IEEE Signal Processing Magazine 8*, 14–38.

SAMSON, J. C. (1977), *Matrix and Stokes Velocity Representations of Detectors for Polarized Waveforms: Theory, with Some Applications to Teleseismic Waves*, Geophys. J. Roy. Astr. Soc. *51*, 583–603.

SOMA, N. (1998), *Evaluation of Deep Geothermal Reservoir Structure by Means of a Reflection Method Using Acoustic Emission*, Doctoral Thesis, Graduate School of Tohoku University (in Japanese).

SOMA, N. and NIITSUMA, H. (1997), *Identification of Structures within the Deep Geothermal Reservoir of the Kakkonda Field, Japan, by a Reflection Method Using Acoustic Emission as a Wave Source*, Geothermics *26*, 43–64.

SOMA, N., NIITSUMA, H., and BARIA, R. (1997), *Estimation of Deeper Structure at the Soultz Hot Dry Rock Field by Means of Reflection Method Using 3C AE as Wave Source*, Pure appl. geophys. *150*, 661–676.

(Received May 5, 2000, revised/accepted November 3, 2000)